Hexatic and fat-fractal structures for water droplets condensing on oil

A. Steyer,* P. Guenoun, and D. Beysens
Service de Physique de l'Etat Condensé, Centre d'Etudes de Saclay, F-91191 Gif-sur-Yvette CEDEX, France
(Received 13 November 1992)

Experiments on water droplets condensing on a liquid substrate (breath figures) are reported. Attractive capillary interactions between drops lead to the formation of particular two-dimensional structures. An hexatic order with exponent $\eta \approx 0.9$ is observed over a small length scale. At larger length scales the defects in the structure exhibit a fat-fractal distribution with exponent $\beta \approx 3.3$.

PACS number(s): 68.10.−m, 64.70.Dv, 82.70.Kj

INTRODUCTION

When water vapor condenses on a substrate under partial-wetting conditions the drops conform to a pattern (breath figures), for which the geometry can be very rich [1]. We focus here on the case where the substrate is a liquid (paraffin oil). A number of observations concerning the growth and the geometrical characteristics of the droplet pattern have already been reported [1,2]. In particular, the droplets are suspended at the surface of the liquid (Fig. 1) because of a subtle balance between buoyancy, droplet weight, and capillary forces [3]. The oil surface is curved around each droplet and elastic energy is stored. The bending of the substrate causes long-ranged elastic interactions between the drops that are able to aggregate, as observed for small solid spheres at the surface of water [4]. In this paper we report the various patterns that the droplets form under the influence of capillary interactions.

A complete calculation of the dependence of the force on the interdroplet distance is extremely difficult. However, some approximations are valid, such as the Nicolson method [3]. This method applies when the bond number $B_0=(R/l_c)^2$ is small enough. Here R is the radius of the droplet and l_c is the capillary length defined as $l_c=(\sigma/\omega)^{1/2}$, where $\omega=\rho g$ is the specific weight of oil, g being the earth's gravitational acceleration, ρ the absolute oil density, and σ is the oil-air surface tension. In our experiment where the radius of the droplets is of order 10 μm, B_0 is equal to 10^{-4} and hence the use of the Nicolson method is applicable. According to this method the attractive force F between two droplets separated by a distance l is

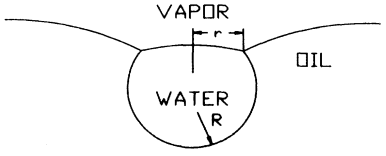

FIG. 1. Water droplet suspended at the surface of oil by means of capillary forces.

$$F=\frac{4\pi R^6\omega^2}{3l\sigma}\left[\frac{1}{d}+0.25(1-p^2)^{1.5}-0.75(1-p^2)^{0.5}\right]^2, \quad (1)$$

where d is the oil-to-air relative density. The quantity p is a key parameter and is defined as the ratio of the apparent drop radius (r) above the surface, to the drop radius (R) below the surface (Fig. 1). This parameter p is related to the contact angles of the drop with the surface and is therefore very sensitive to the wetting properties of the oil-water interface. By varying p the force can be magnified by two orders of magnitude. Since the interaction force can be directly deduced from Eq. (1), the parameter p, which can be easily determined by microscope observation, can be used as a quantitative measurement of the interaction between the drops. Note that any temperature gradient around a drop would be of radial symmetry and thus will not affect Eq. (1).

EXPERIMENT

A flow of nitrogen gas saturated with water is passed onto the surface of paraffin oil. The gas is at room temperature (23±0.3°C) and oil is maintained at 5°C to within 0.1°C. Water droplets nucleate and grow at the oil surface. These droplets attract each other as described above. When two droplets touch each other, they do not coalesce due to the presence of a film of oil at the contact point [2]. In fact, the droplets stay in contact during the course of the experiment. Note that the link between the drops is not rigid; one droplet can easily slide around another droplet. When more than two droplets are in contact, they can rearrange themselves to reach a more stable configuration in two dimensions, which is the compact hexagonal structure. We indeed observe islands of droplets that are arranged in such a structure (Fig. 2). The islands, in turn, attract each other in a much stronger way than the single droplets. This is because the attractive force between the islands is proportional to the sixth power of their radii as in Eq. (1). After they collide, the islands rotate around the point of contact in order to minimize the elastic energy. This is made possible because the friction between the droplets is negligible. As a consequence, the orientation of the hexagonal structure is

1063-651X/93/48(1)/428(4)/$06.00

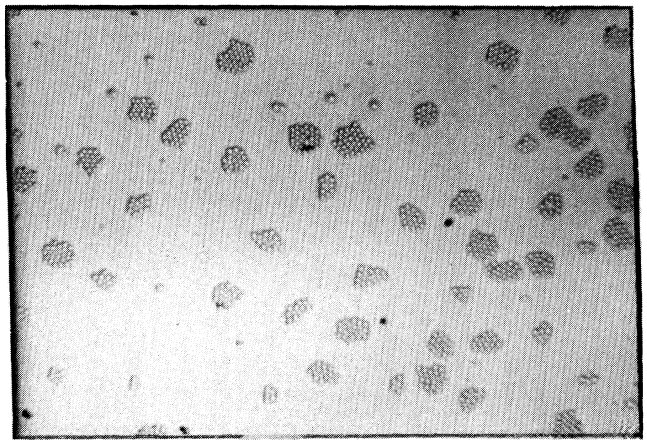

FIG. 2. Formation of islands at the beginning of the vapor deposition. The smallest dimension of the picture corresponds to 650 μm.

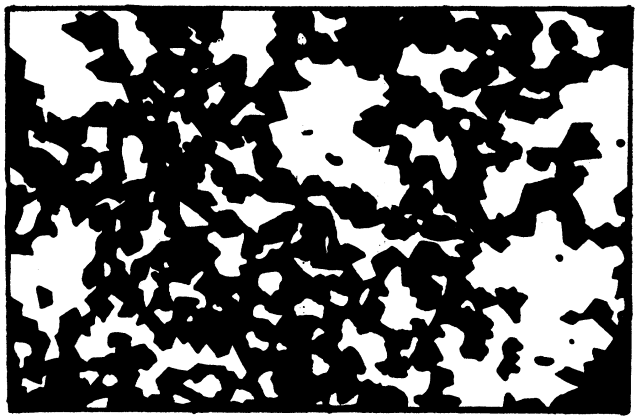

FIG. 4. Fat-fractal structure that has been emphasized by coloring in black (white) the zones with (without) droplets. The smallest dimension of the picture corresponds to 650 μm.

not very different from one island to the other (Fig. 3), and we will see further that an hexatic phase can be found in such a stage of aggregation. However, if one looks at a larger scale, one can see a large number of holes in the pattern. This is shown in Fig. 4 where the regions filled with droplets have been blackened and the empty zones whitened. The formation of holes is unavoidable because the islands are too densely packed to rotate freely. These holes have a fractal-like geometry. In fact we show below that the holes can be described as fat fractals.

All the patterns that we have described until now (hexatic and fat fractal) are not observed on the whole oil surface. In some places the interaction between the droplets is not large enough to create islands; the pattern is only weakly ordered. This case has been considered in detail elsewhere [2]. One can ask why, in the same experiment, there are regions where droplets form hexatic patterns and other regions where they do not. The answer lies in the variations of the parameter p, whose value ranges from 0.4 to 0.8 in the hexatic zones and from 0.2 to 0.4 in the rest. This means that the force between the drops is 60% higher in the hexatic zones. Although the inhomogeneity in the interaction explains the inhomogeneity in the patterns, the physical origin of the difference is not well understood. We suggest that impurities in water and oil could be the cause. The parameter p is an increasing function of σ, the oil-air interfacial tension, which is known to decrease drastically with contaminants, acting as surfactants. Indeed, experiment performed under very clean conditions, where σ is large, greatly facilitates the formation of hexatic zones.

We now present a quantitative analysis of the patterns.

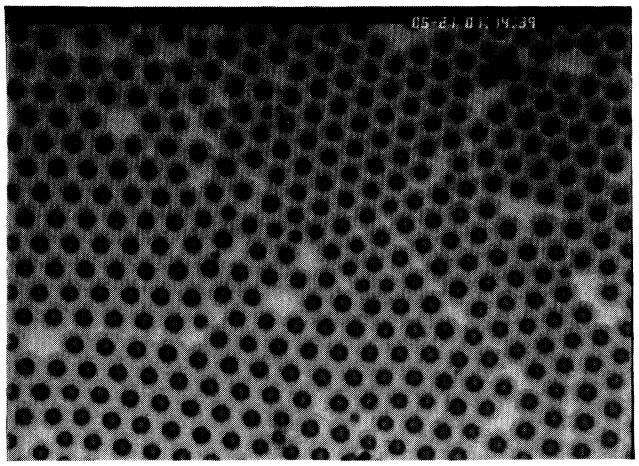

FIG. 3. Islands that have merged. The smallest dimension of the picture corresponds to 350 μm.

HEXATIC PHASE

We consider the hexatic phase only as a geometrical way to characterize a two-dimensional assembly of points. The complete theory by Nelson *et al.* [5] is not relevant to our system, where no quantity equivalent to temperature is explicitly available. In the following we will only consider in their model the geometrical approach where an hexatic phase is a two-dimensional pattern with long-range orientational correlations. One can prove the hexatic order by considering the spatial correlation function of the order parameter

$$G_6(r)=\langle \exp(6i\theta(r)) \rangle \ , \tag{2}$$

where $i=\sqrt{-1}$ and $\theta(r)$ is the angle (with respect to some fixed direction) of the segment between two neighboring droplets whose centers are separated by r. The averaging procedure denoted by $\langle\ \rangle$ is performed over the different droplets. In an hexatic phase, $G_6(r)$ decreases as $r^{-\eta}$ (η is an exponent that we discuss below), whereas G_6 is exponentially decaying in a random structure.

We have determined the G_6 function from the experiments by using an image-processing system. In order to determine which drops are neighbors, we used a method based on Voronoi polygons. Such a polygon is the smallest convex polygon surrounding a drop whose sides are

the bisectors of the lines between the drops and its neighbors. Two drops are said to be neighbors if their respective Voronoi polygons have one side in common. The result is shown in Fig. 5. The range over which the hexatic order extends is of order 10 drops, which is close to the diameter of the islands. This shows that the orientational order persists only from one island to the nearest-neighbor island.

The measured value of the exponent η is always close to 0.9. This value can be interpreted in terms of structural defects according to Ref. 2. With c the concentration of defects in the structure, it can be shown [5] that

$$\eta = 9c/\pi \ . \tag{3}$$

The concentration c can be deduced from the Voronoi polygons as the fraction of polygons that do not have six sides. By using the same technique as in Ref. [2] we obtain $c \approx 0.35$, in close agreement with the value (0.32) deduced from η. The large value of η is thus the consequence of the large number of defects in the pattern.

FAT FRACTAL

We consider now a larger scale where droplets are not resolved. At this scale, the holes can be clearly identified as shown in Fig. 4. We want to quantify their distribution.

Umberger and Farmer [6] have proposed a new definition for fractal objects of nonzero surface, called fat fractal. The relevant exponent (β) for such structures with holes can be obtained as follows. Let us consider $S(R_g)$, the total surface of these holes which have a radius of gyration smaller than the length R_g. The radius of gyration of a hole is defined as $R_g = \sum_i [(x_i - x_g)^2 + (y_i - y_g)^2]^{1/2}$ where x_i and y_i are the coordinates of an element i of the hole and x_g and y_g are the coordinates of the center of mass of the hole. Then β is defined as the limit of the ratio $\ln[S(R_g)]/\ln(R_g)$ when R_g becomes small. Experimentally, we use a two-step method to determine β. First, we consider the relationship between the surface S of the holes and their radius R_g (Fig. 6). For the ten different patterns that we have analyzed we find that the data can be fitted to the power law

$$S(R_g) \sim R_g^{\delta} \ . \tag{4}$$

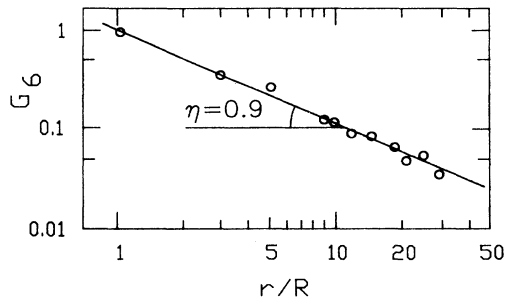

FIG. 5. 60° angle orientation correlation function (G_6) as a function of the distance r in a log-log plot. r is expressed in units of R, the radius of the drops (10 μm in this experiment).

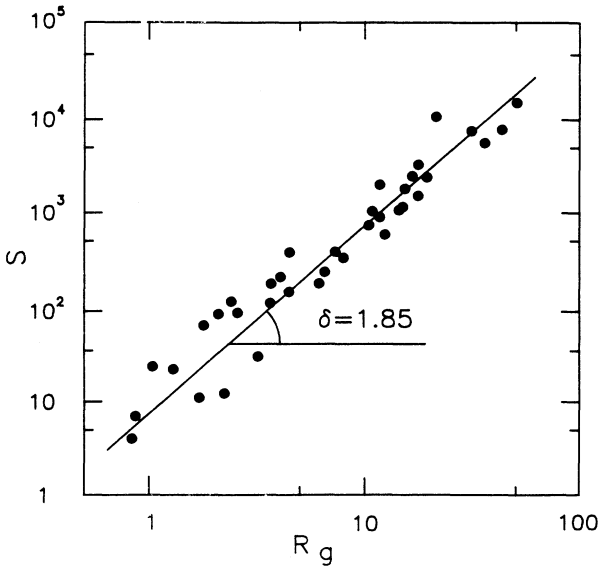

FIG. 6. Surface S of holes vs the hole gyration radius R_g in a log-log plot. R_g is expressed in units of R, the radius of the drops (typically 10 μm).

Here, $\delta = 1.85 \pm 0.25$ (the uncertainty corresponds to two standard deviations). The fact that δ is close to 2 is a mere consequence of compact holes. Second, we calculate the size distribution function $F(R_g)$ of the holes (Fig. 7), which is the number of holes whose radius of gyration is less than R_g. For holes that are not too large we find

$$F(R_g) \sim R_g^{\alpha} \ , \tag{5}$$

with the exponent $\alpha = 1.4 \pm 0.1$ (two standard deviations). This law breaks down for large values of R_g because of the finite size of the analyzed picture. The power laws [Eqs. (4) and (5)] confirm that the patterns observed in breath figures are fat fractals. One can easily deduce now from the definitions of β, δ, and α that $\beta = \delta + \alpha = 3.30 \pm 0.35$. This value, which characterizes

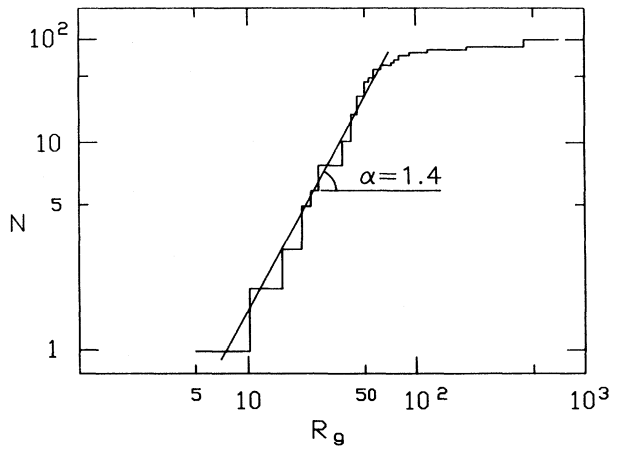

FIG. 7. Number of holes of size smaller than R_g in a log-log plot. R_g is expressed in units of R, the radius of the drops (typically 10 μm).

the structure of the pattern, should not be compared with the space dimensionality.

CONCLUDING REMARKS

Breath figures appear to be a very convenient way for generating various two-dimensional structures such as hexatic phases, fractals, or other less-ordered patterns [2]. More than a simple model, breath figures offer a number of interesting features. The first interesting feature is the negligible friction between drops. This allows many rearrangements in the global structure to occur and leads to a pattern—a fat fractal—which is more compact than a classical fractal. The possibility for rearrangements also leads to the persistence of an orientational order of about the size of an island and to an hexatic order. The second interesting aspect is the possibility of observing hexatic and fractal patterns simultaneously. Furthermore, we find a quantitative link between the two structures: the more fractal the structure, the less long-ranged the hexatic order. One can imagine two extreme situations, one being a large hexatic phase with a few holes in it. Then the exponent η is small and β cannot be determined. The second case is a pattern similar to classical branched fractals with no orientational order. The breath-figure experiments on liquids provide patterns that are in between these two extreme cases. It would be of interest to obtain the numerical values of η and β from the numerical simulation of interacting drops and compare with the experiments. However, the physicochemical origin of the inhomogeneities in the capillary interactions still remains unclear. This aspect deserves further studies.

ACKNOWLEDGMENTS

We are grateful to M. Cloitre and J. Van Duijneveldt for very fruitful discussions and to A. Engelman and A. Stegner for their help in the measurements.

---

*Present address: Ecole Nationale des Télécommunications, F-75013 Paris, France.

[1] See, e.g., D. Beysens, A. Steyer, P. Guenoun, D. Fritter, and C. M. Knobler, Phase Transitions **31**, 219 (1991), and references cited therein.

[2] A. Steyer, P. Guenoun, D. Beysens, and C. M. Knobler, Phys. Rev. B **42**, 1086 (1990), and references cited therein.

[3] M. M. Nicolson, Proc. Cambridge Philos. Soc. **45**, 288 (1949); D. Y. C. Chan, J. D. Henry, and L. R. White, J. Colloid Interface Sci. **79**, 410 (1981).

[4] C. Allain and M. Cloitre, Ann. Phys. **13**, 141 (1988).

[5] D. R. Nelson, M. Rubinstein, and F. Spaepen, Philos. Mag. A **46**, 105 (1982).

[6] D. K. Umberger and J. D. Farmer, Phys. Rev. Lett. **55**, 661 (1985).

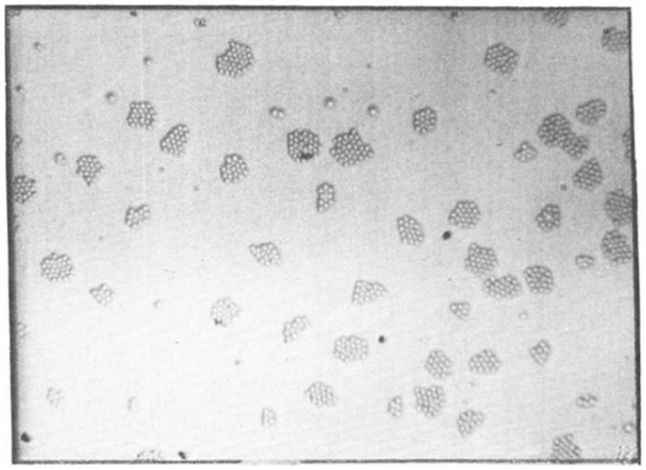

FIG. 2. Formation of islands at the beginning of the vapor deposition. The smallest dimension of the picture corresponds to 650 μm.

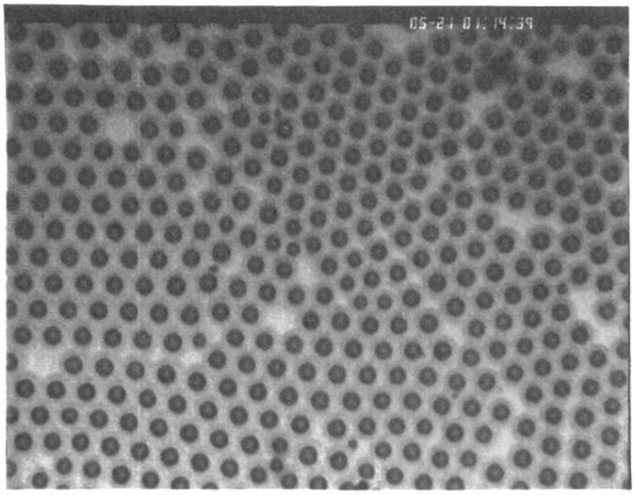

FIG. 3. Islands that have merged. The smallest dimension of the picture corresponds to 350 μm.